A RATIONAL DESIGN OF A DIGITAL SHEARLET TRANSFORM

David L. Donoho[1], *Gitta Kutyniok*[2], *Morteza Shahram*[1], *and Xiaosheng Zhuang*[2]

[1]Department of Statistics, Stanford University, Stanford, CA 94305, USA
[2]Institute of Mathematics, University of Osnabrück, 49069 Osnabrück, Germany
Emails: {donoho, mshahram}@stanford.edu; {kutyniok,xzhuang}@uni-osnabrueck.de

ABSTRACT

In this paper, we first develop a digital shearlet theory which is rationally designed in the sense that it is the digitalization of the existing shearlet theory for continuum data. This shows that shearlet theory indeed provides a unified treatment for the continuum and digital realm. Secondly, we discuss our implementation of the associated digital shearlet transform. This software package called ShearLab is also rationally designed by providing various performance measures quantifying precision of the reconstruction, tightness of the frame, robustness of the shearlet transform, and other properties. Such quantitative performance metrics allow us to tune parameters and objectively improve our implementation as well as compare different directional transform implementations.

Keywords— Digital shearlet theory, Parabolic Scaling, Pseudo-Polar Grid, Shearlets, Test Measures.

1. INTRODUCTION

Wavelets are nowadays indispensable as a multiscale encoding system for a wide range of more theoretically to more practically oriented tasks, since they provide optimal approximation rates for smooth 1-dimensional functions/signals exhibiting singularities. Also the fact that they provide a unified treatment in both the continuum as well as digital setting was essential for their success. It can however be shown that wavelets – although perfectly suited for isotropic structures – do not perform equally well when dealing with anisotropic phenomena.

This fact has motivated the development of various types of directional representation systems for 2-dimensional signals (continuous and digital), e.g., [2, 3], that are capable of resolving edge- or curve-like features which separate smooth regions in a precise and more economical (sparse) way. Among all these systems, the shearlet system (see [5, 6]) is the first directional representation system which – in addition to the aforementioned favorable properties – provides a unified treatment for the continuum and digital world similar to wavelets.

In this paper, we will make the notion of a digital shearlet transform precise. We will accompany our theoretical considerations with a publicly available software-package called ShearLab, thereby also supporting the philosophy of 'reproducible research' [4]. In addition, we provide an extensive testing package, which firstly shows the performance of our algorithm, and secondly shall serve the community as performance measures to allow a precise comparison with future implementations. All presented algorithms and tests as well as codes for the displayed figures and tables are provided at URL `ShearLab.org`.

This work was partially supported by DFG Heisenberg Fellowship KU 1446/8 as well as DFG Grants KU 1446/13 and KU 1446/14.

2. THE DIGITAL SHEARLET TRANSFORM

In this section, we will introduce the digital shearlet transform (DShT) of an $N \times N$ image, which cascades the following steps:

1) Pseudo-polar transform with oversampling factor of R (we choose $R = 8$ in this paper) in the radial direction.
2) Multiplication by 'density-compensation-style' weights.
3) Decomposing the pseudo-polar-indexed array into rectangular subbands with additional 2D-iFFT.

This is an exact analogy of the continuum domain shearlet transform [5]. With a careful choice of the weights and the windows, this transform is an isometry. Then the inverse transform can be computed by merely taking the adjoint in each step.

2.1. Weighted Pseudo-Polar Transforms

To address 1) and 2), given an $N \times N$ image I, our goal is to choose weights $w : \Omega_R \to \mathbb{R}^+$ so that

$$\sum_{u,v=-N/2}^{N/2-1} |I(u,v)|^2 = \sum_{(\omega_x,\omega_y)\in\Omega_R} \omega(\omega_x,\omega_y) \cdot |\hat{I}(\omega_x,\omega_y)|^2, \quad (1)$$

where $\hat{I}(\omega_x, \omega_y)$ is the pseudo-polar Fourier transform given by

$$\hat{I}(\omega_x,\omega_y) = \sum_{u,v=-N/2}^{N/2-1} I(u,v) e^{-\frac{2\pi i}{RN+1}(u\omega_x + v\omega_y)}$$

and $\Omega_R = \Omega_R^1 \cup \Omega_R^2$ is the pseudo-polar grid with

$$\begin{aligned} \Omega_R^1 &= \{(-\tfrac{4\ell k}{RN}, \tfrac{2k}{R}) : -\tfrac{N}{2} \le \ell \le \tfrac{N}{2}, -\tfrac{RN}{2} \le k \le \tfrac{RN}{2}\}, \\ \Omega_R^2 &= \{(\tfrac{2k}{R}, -\tfrac{4\ell k}{RN}) : -\tfrac{N}{2} \le \ell \le \tfrac{N}{2}, -\tfrac{RN}{2} \le k \le \tfrac{RN}{2}\}, \end{aligned}$$

and $R \ge 2$ is the oversampling factor. These grids are illustrated in Figure 1. Notice that the center $\mathcal{C} = \{(0,0)\}$ appears $N+1$ times in Ω_R^1 and Ω_R^2, and the points on the seam

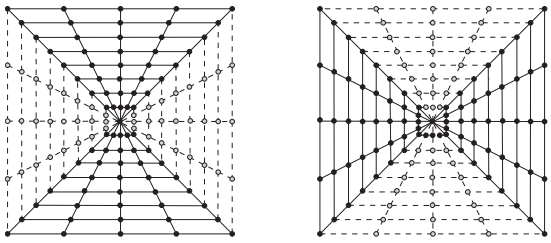

Ω_R^1 Ω_R^2

Fig. 1. The pseudo-polar grid for $N = 4$ and $R = 4$.

lines $\mathcal{S}_R^1 = \{(-\frac{2k}{R}, \frac{2k}{R}) : -\frac{RN}{2} \le k \le \frac{RN}{2}, k \ne 0\}$ and $\mathcal{S}_R^2 = \{(\frac{2k}{R}, -\frac{2k}{R}) : -\frac{RN}{2} \le k \le \frac{RN}{2}, k \ne 0\}$ appear in both Ω_R^1 and Ω_R^2. Choosing the weights carefully, the following 'Plancherel theorem' – similar to the one for the discrete Fourier transform – can be proved for the pseudo-polar grid $\Omega_R = \Omega_R^1 \cup \Omega_R^2$.

Theorem 1 *Let N be even, and let $w : \Omega_R \to \mathbb{R}^+$ be a weight function. Then* (1) *holds if and only if, for all $-N+1 \le u, v \le N-1$, the weights w satisfy*

$$\begin{aligned}\delta(u,v) &= w(0,0) \\ &+ 4 \sum_{\ell=0,N/2} \sum_{k=1}^{RN/2} w(\tfrac{2k}{R}, -\tfrac{4\ell k}{RN}) \cos(\tfrac{2ku}{R(RN+1)}) \cos(\tfrac{4\ell kv}{RN(RN+1)}) \\ &+ 8 \sum_{\ell=1}^{N/2-1} \sum_{k=1}^{RN/2} w(\tfrac{2k}{R}, -\tfrac{4\ell k}{RN}) \cos(\tfrac{2ku}{R(RN+1)}) \cos(\tfrac{4\ell kv}{RN(RN+1)})\end{aligned}$$

and, for all $(\omega_x, \omega_y) \in \Omega_R$, the weights w satisfy the symmetry conditions $w(\omega_x, \omega_y) = w(\omega_y, \omega_x)$, $w(\omega_x, \omega_y) = w(-\omega_x, \omega_y)$, and $w(\omega_x, \omega_y) = w(\omega_x, -\omega_y)$.

2.2. Recommended Choice of Weights

To avoid high complexity in the computation of the weights satisfying Theorem 1, we relax the requirement for exact isometric weighting, however instead represent the weights not as the solution of a large system of equations, but in terms of an undercomplete basis for functions on the pseudo-polar grid. We compute the coefficients in this expansion once for a given problem size; then hardwire them in the algorithm. For the present algorithm, we expand using 7 functions $w_1, \dots, w_7$ on the pseudo-polar grid such that $\sum_{j=1}^7 w_j(\omega_x, \omega_y) \ne 0$ for each $(\omega_x, \omega_y) \in \Omega_R$:

Center: $w_1 = 1_{(0,0)}$ and $w_2 = 1_{\{(\omega_x,\omega_y):|k|=1\}}$,
Boundary: $w_3 = 1_{\{(\omega_x,\omega_y):|k|=NR/2,\, \omega_x=\omega_y\}}$ and $w_4 = 1_{\{(\omega_x,\omega_y):|k|=NR/2,\, \omega_x\ne\omega_y\}}$,
Seam lines: $w_5(\omega_x, \omega_y) = |k| \cdot 1_{\{(\omega_x,\omega_y):1<|k|<NR/2,\, \omega_x=\omega_y\}}$ and $w_6 = 1_{\{(\omega_x,\omega_y):|k|=NR/2-3,\, \omega_x=\omega_y\}}$,
Interior: $w_7(\omega_x, \omega_y) = |k| \cdot 1_{\{(\omega_x,\omega_y):1<|k|<NR/2,\, \omega_x\ne\omega_y\}}$.

Notice that here we use (ω_x, ω_y) and (k, ℓ) interchangeably. The weighting generated by our recommended choice of coefficients for $w_1, \dots, w_7$ is displayed in Figure 2.

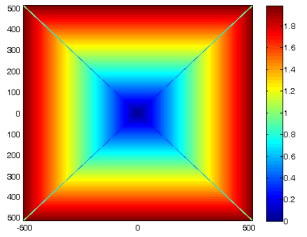

Fig. 2. Recommended weighting of the pseudo-polar grid.

2.3. Digital Shearlets on the Pseudo-Polar Grid

To detail 3), let W_0 be the Fourier transform of the Meyer scaling function satisfying supp $W_0 \subseteq [-4^{j_R}, 4^{j_R}]$ with $j_R := -\lceil \log_4(R/2) \rceil$, and let V_0 be a 'bump function' satisfying supp $V_0 \subseteq [-4^{j_R} - 1/2, 4^{j_R} + 1/2]$ with $V_0(x) \equiv 1$ for $|x| \le 4^{j_R}$, for which numerous choices exist. Then we define the scaling function ϕ for the digital shearlet system to be

$$\hat{\phi}(\xi_1, \xi_2) = W_0(\xi_1) V_0(\xi_2), \quad (\xi_1, \xi_2) \in \mathbb{R}^2.$$

We further choose W to be the Fourier transform of the Meyer wavelet function satisfying supp $W \subseteq [-4^{j_R+1}, -4^{j_R-1}] \cup [4^{j_R-1}, 4^{j_R+1}]$, and V to be a 'bump' function satisfying supp $V \subseteq [-1, 1]$ and $|V(\xi - 1)|^2 + |V(\xi)|^2 + |V(\xi + 1)|^2 = 1$ for all $|\xi| \le 1$ and $\xi \in \mathbb{R}$. Then the generating shearlet ψ for the digital shearlet system on Ω_R^2 is defined as

$$\hat{\psi}(\xi_1, \xi_2) = W(\xi_1) V(\tfrac{\xi_2}{\xi_1}), \quad (\xi_1, \xi_2) \in \mathbb{R}^2.$$

Before stating the definition of digital shearlets, we first partition the set Ω_R beyond the already defined partitioning into Ω_R^1 and Ω_R^2 by setting $\Omega_R^1 = \Omega_R^{11} \cup \mathcal{C} \cup \Omega_R^{12}$ and $\Omega_R^2 = \Omega_R^{21} \cup \mathcal{C} \cup \Omega_R^{22}$, where

$$\begin{aligned}\Omega_R^{11} &= \{(-\tfrac{4\ell k}{RN}, \tfrac{2k}{R}) : -\tfrac{N}{2} \le \ell \le \tfrac{N}{2}, 1 \le k \le \tfrac{RN}{2}\}, \\ \Omega_R^{12} &= \{(-\tfrac{4\ell k}{RN}, \tfrac{2k}{R}) : -\tfrac{N}{2} \le \ell \le \tfrac{N}{2}, -\tfrac{RN}{2} \le k \le -1\}, \\ \Omega_R^{21} &= \{(\tfrac{2k}{R}, -\tfrac{4\ell k}{RN}) : -\tfrac{N}{2} \le \ell \le \tfrac{N}{2}, 1 \le k \le \tfrac{RN}{2}\}, \\ \Omega_R^{22} &= \{(\tfrac{2k}{R}, -\tfrac{4\ell k}{RN}) : -\tfrac{N}{2} \le \ell \le \tfrac{N}{2}, -\tfrac{RN}{2} \le k \le -1\}.\end{aligned}$$

The number of sampling points in radial and angular direction affected by a window at scale j and shear s is now given by

$$\mathcal{L}_j^1 = \begin{cases} 4^{j+j_R-1} \frac{R}{2} 15 + 1 & : 0 \le j < \lceil \log_4 N \rceil - j_R, \\ \lfloor \frac{R}{2}(N - 4^{j+j_R-1}) \rfloor + 1 & : j = \lceil \log_4 N \rceil - j_R, \end{cases}$$

and

$$\mathcal{L}_{j,s}^2 = \begin{cases} 2^{-j} N + 1 & : -2^j < s < 2^j, \\ 2^{-j} \frac{N}{2} + 1 & : s \in \{-2^j, 2^j\}. \end{cases}$$

We further define $\mathcal{R}_{j,s}$ to be a rectangle given by

$$\begin{aligned}\mathcal{R}_{j,s} = \{&((\mathcal{L}_j^1)^{-1} 4^j (R/2) r_1, -(\mathcal{L}_{j,s}^2)^{-1} (N/2^{j+1}) r_2) : \\ &r_1 = 0, \dots, \mathcal{L}_j^1 - 1,\ r_2 = 0, \dots, \mathcal{L}_{j,s}^2 - 1\},\end{aligned}$$

and choose the low frequency rectangle to be

$$\mathcal{R} = \{(r_1, r_2) : r_1 = -1, \dots, 1,\ r_2 = -\frac{N}{2}, \dots, \frac{N}{2}\}.$$

We are now ready to define digital shearlets.

Definition 1 *At scale $j \in \{0, \dots, \lceil \log_4 N \rceil - j_R\}$, shear $s = \{-2^j, \dots, 2^j\}$, and spatial position $m \in \mathcal{R}_{j,s}$, the* digital shearlets *on the cone Ω_R^2 are defined by*

$$\sigma^{21}_{j,s,m}(\omega_x, \omega_y) = \frac{C(\omega_x, \omega_y)}{\sqrt{|\mathcal{R}_{j,s}|}} W(4^{-j}\omega_x)\, V(s + 2^j \tfrac{\omega_y}{\omega_x}) \cdot \chi_{\Omega_R^{21}}(\omega_x, \omega_y)\, e^{-2\pi i m'(4^{-j}\frac{2k}{R}, -2^{j+1}\frac{\ell}{N})},$$

where

$$C(\omega_x, \omega_y) = \begin{cases} 1 & : \ (\omega_x, \omega_y) \notin \mathcal{S}_R^1 \cup \mathcal{S}_R^2, \\ \frac{1}{\sqrt{2}} & : \ (\omega_x, \omega_y) \in (\mathcal{S}_R^1 \cup \mathcal{S}_R^2) \setminus \mathcal{C}, \\ \frac{1}{\sqrt{2(N+1)}} & : \ (\omega_x, \omega_y) \in \mathcal{C}. \end{cases}$$

The shearlets $\sigma^{11}_{j,s,m}, \sigma^{12}_{j,s,m}, \sigma^{22}_{j,s,m}$ on the remaining cones are defined accordingly by symmetry with equal indexing sets. For $n \in \mathcal{R}$, we further define the functions

$$\varphi^{\iota}_n(\omega_x, \omega_y) = \frac{C(\omega_x, \omega_y)}{\sqrt{|\mathcal{R}|}} W_0(\omega_x)\, V_0(\omega_y) \cdot \chi_{\Omega_R^{21}}(\omega_x, \omega_y)\, e^{-in'(\frac{k}{3}, \frac{\ell}{N+1})}, \ \iota = 1, 2.$$

Summarizing, we call the system

$$\{\varphi^{\iota}_n : \iota = 1, 2, n \in \mathcal{R}\} \cup \{\sigma^{11}_{j,s,m}, \sigma^{12}_{j,s,m}, \sigma^{21}_{j,s,m}, \sigma^{22}_{j,s,m} : j \in \{0, \dots, \lceil \log_4 N \rceil - j_R\}, s = \{-2^j, \dots, 2^j\}, m \in \mathcal{R}_{j,s}\}$$

the digital shearlet system*, and denote it by $\mathcal{DSH}$.*

This system has the following desirable property:

Theorem 2 *The digital shearlet system $\mathcal{DSH}$ defined in Definition 1 forms a tight frame for functions $f : \Omega_R \to \mathbb{C}$.*

3. QUANTITATIVE TEST MEASURES

We now introduce several performance measures, which shall provide a means to quantify the performance of our algorithm, a framework for tuning and improving our algorithm, and a basis for comparison of all parabolic scaling algorithms.

In the following, P shall denote the pseudo-polar transform, w the weighting on the pseudo-polar grid, W the windowing with additional iFFT, and $S = W\sqrt{w}P$ the shearlet transform.

[D1] *Algebraic Exactness.* We require the transform to be the precise implementation of a theory for digital data on a pseudo-polar grid. Our quality measure for this will be the Monte Carlo estimate for the operator norm $\|W^\star W - Id\|_{op}$ given by $M_{alg} = \max_{i=1,\dots,5} \frac{\|W^\star W J_i - J_i\|_2}{\|J_i\|_2}$, where $\{J_i : i = 1, \dots, 5\}$ is a sequence of 5 random images on a pseudo-polar grid for $N = 512$ and $R = 8$ with standard normally distributed entries.

[D2] *Isometry of Pseudo-Polar Transform.* To measure the closeness to being an isometry, let $I_1, \dots, I_5$ be 5 random images $I_1, \dots, I_5$ of size 512×512 with standard normally distributed entries. Then we define the following measures:

- Closeness to tightness. Our quality measure will here be the Monte Carlo estimate for the operator norm $\|P^\star w P - Id\|_{op}$ given by $M_{isom_1} = \max_{i=1,\dots,5} \frac{\|P^\star w P I_i - I_i\|_2}{\|I_i\|_2}$.
- Quality of preconditioning. Our quality measure will be the spread of the eigenvalues of the Gram operator $P^\star w P$ given by $M_{isom_2} = \frac{\lambda_{\max}(P^\star w P)}{\lambda_{\min}(P^\star w P)}$.
- Invertibility. Our quality measure will be the Monte Carlo estimate for the invertibility of the operator $\sqrt{w}P$ using conjugate gradient method $G_{\sqrt{w}P}$ (residual error is set to be 10^{-6}) given by $M_{isom_3} = \max_{i=1,\dots,5} \frac{\|G_{\sqrt{w}P}\sqrt{w}P I_i - I_i\|_2}{\|I_i\|_2}$.

We expect a trade-off between the oversampling rate and the closeness to being an isometry. Note that we do not take the oversampling rate into account in these measures, but would like to mention that this rate will instead affect the measure for speed [D4].

[D3] *Tight Frame Property.* We now combine [D1] and [D2] to allow comparison with other transforms. Let $I_1, \dots, I_5$ be a sequence of 5 random images of size 512×512 with standard normally distributed entries. Our quality measure will be the Monte Carlo estimate for $\|S^\star S - Id\|_{op}$ given by $M_{tight_1} = \max_{i=1,\dots,5} \frac{\|S^\star S I_i - I_i\|_2}{\|I_i\|_2}$ as well as using conjugate gradient $G_{\sqrt{w}P}$ given by $M_{tight_2} = \max_{i=1,\dots,5} \frac{\|G_{\sqrt{w}P} W^\star S I_i - I_i\|_2}{\|I_i\|_2}$.

[D4] *Speed.* We test the speed up to a size of $N = 1024$ which will be enough for computing the complexity of our algorithm. Generate a sequence of 6 random images I_i, $i = 5, \dots, 10$ of size $2^i \times 2^i$ with standard normally distributed entries. Let s_i be the speed of S applied to I_i. Our hypothesis is that the speed behaves like $s_i = c \cdot (2^{2i})^d$. To introduce appropriate measures, let $\tilde{d}_a$ be the average slope of the line, which is a least square fit to the curve $i \mapsto \log(s_i)$, and let f_i be the 2D-FFT applied to I_i. Our quality measure will then be three-fold:

- Complexity: $M_{speed_1} = \frac{\tilde{d}_a}{2 \log 2}$.
- The Constant: $M_{speed_2} = \frac{1}{6} \sum_{i=5}^{10} \frac{s_i}{(2^{2i})^{M_{speed,1}}}$.
- Comparison with 2D-FFT: $M_{speed_3} = \frac{1}{6} \sum_{i=5}^{10} \frac{s_i}{f_i}$.

[D5] *Robustness.* We will analyze two different types of robustness which we believe are the most common impacts on a sequence of transform coefficients. Let I be the regular 512×512 sampling of a Gaussian function with mean 0 and variance 512 on $\{-256, 255\}^2$. Then we consider the resilience to

- Thresholding. Our quality measure will be the curve $M_{thres_{k,p_k}} = \frac{\|G_{\sqrt{w}P} W^\star \operatorname{thres}_{k,p} S I - I\|_2}{\|I\|_2}, k = 1, 2,$ where $\operatorname{thres}_{1,p_1}$ discards $100 \cdot (1 - 2^{-p_1})$ percent of the coefficients ($p_1 = [2 : 2 : 10]$) and $\operatorname{thres}_{2,p_2}$

sets all those coefficients to zero with absolute values below the threshold $m(1-2^{-p_2})$ with m being the maximal absolute value of all coefficients ($p_2 = [0.001 : 0.01 : 0.05]$).

- Quantization. Our quality measure will be $M_{quant,q} = \frac{\|G_{\sqrt{w}P} W^\star \operatorname{quant}_q SI - I\|_2}{\|I\|_2}$, where $q = [8 : -0.5 : 6]$ and $\operatorname{quant}_q(c) = \operatorname{round}(c/(m/2^q)) \cdot (m/2^q)$.

4. TEST RESULTS

In this section, we provide numerical results for the quantitative measures in [D1]–[D5] of our present implementation.

4.1. Results for Tests [D1]–[D3]

Table I presents the performance with respect to the quantitative measures in [D1]–[D3].

TABLE I. RESULTS FOR [D1]–[D3]

M_{alg}	M_{isom_1}	M_{isom_2}	M_{isom_3}	M_{tight_1}	M_{tight_2}
6.6E-16	0.017	1.762	3.3E-7	0.017	3.8E-7

The quantity $M_{alg} \approx$ 6.6E-16 confirms that the $\mathcal{DSH}$ is indeed up to machine precision a tight frame. The tightness deficiency of $M_{tight_1} \approx 0.017$ (also $M_{isom_1} \approx 0.017$) mainly results from the isometry deficiency of the weighting. Evidently, progress on the choice of weights could have a significant impact on this error. Further, note that the condition number ($M_{isom_2} \approx 1.762$) of the Gram matrix is quit close to 1, which allows us to employ the conjugate gradient method very efficiently to compute the inverse of the shearlet transform S ($M_{isom_3} \approx$ 3.3E-7 and $M_{tight_2} \approx$ 3.8E-7). Observe that there is a trade-off between the sophistication of the weights, the running time of S, and the smoothness of the shearlets.

4.2. Timing Test [D4]

The timing performance measuring the complexity M_{speed_1}, the constant M_{speed_2}, and the comparison with 2D-FFT M_{speed_3} are presented in Table II.

TABLE II. RESULTS FOR [D4]

M_{speed_1}	M_{speed_2}	M_{speed_3}
0.402	1.028	202.693

Superficially, these measures would seem to say that our implementation has *sublinear* running time characteristics, scaling approximately as N, for an $N \times N$ image. However, we believe this is simply a start-up effect caused by the significant overhead that the implementation imposes on very small problems, which becomes less important for large problems. For the same reason, we don't believe that the factor of 202 comparison to running time of the FFT adequately describes the comparison for large problem sizes N; the comparison gets much more favorable to the DShT as N grows large.

4.3. Robustness Test [D5]

Table III presents the measurements concerning [D5].

TABLE III. RESULTS FOR [D5]

$M_{thres_{1,p_1}}$	1.5E-8	7.2E-8	2.5E-5	0.001	0.007
$M_{thres_{2,p_2}}$	0.005	0.039	0.078	0.113	0.154
$M_{quant,q}$	0.034	0.047	0.057	0.071	0.109

This shows that even if we discard $100(1-2^{-10}) \approx 99.9\%$ of the shearlet coefficients, the original image is still well approximated by the reconstructed image ($M_{thres_{1,p_1}} \approx 0.007$). Thus the number of the significant coefficients is relative small compared to the total number of shearlet coefficients. By the second row, knowledge of the shearlet coefficients with absolute value greater than $m(1-1/2^{0.001})$ ($\approx 0.1\%$ of coefficients) is sufficient for precise reconstruction ($M_{thres_{1,p_2}} \approx 0.005$). The quantization test $M_{quant,q}$ shows the high resilience of the DShT with respect to even quite coarse quantization.

5. CONCLUSIONS

We have developed and implemented a digital shearlet transform based on a carefully designed digital shearlet theory, which is the natural digitization of the continuum shearlet transform. We further defined performance measures which could be used to study not only our, but indeed any digital implementation of a general parabolic scaling algorithm.

6. REFERENCES

[1] A. Averbuch, R. R. Coifman, D. L. Donoho, M. Israeli, and Y. Shkolnisky, *A framework for discrete integral transformations I – the pseudo-polar Fourier transform*, SIAM J. Sci. Comput. **30** (2008), 764–784.

[2] E. J. Candès and D. L. Donoho, *New tight frames of curvelets and optimal representations of objects with C^2 singularities*, Comm. Pure Appl. Math. **56** (2004), 219–266.

[3] M. N. Do and M. Vetterli, *The contourlet transform: an efficient directional multiresolution image representation*, IEEE Trans. Image Process. **14** (2005), 2091–2106.

[4] D. L. Donoho, A. Maleki, M. Shahram, V. Stodden, and I. Ur-Rahman, *Fifteen years of Reproducible Research in Computational Harmonic Analysis*, Comput. Sci. Eng., **11** (2009), 8–18.

[5] K. Guo, G. Kutyniok, and D. Labate, *Sparse Multidimensional Representations using Anisotropic Dilation and Shear Operators*, Wavelets and Splines (Athens, GA, 2005), Nashboro Press, Nashville, TN (2006), 189-201.

[6] G. Kutyniok and D. Labate, *Resolution of the Wavefront Set using Continuous Shearlets*, Trans. Amer. Math. Soc., **361** (2009), 2719–2754.